Trans. JWRI, Vol. 25 (1996), No. 1

Effect of Welding Residual Stresses on Fracture Toughness Testing†

Part 1: FEM Analysis of CTOD Specimens in Multipass Weldments of Thick Plates

Juan C. SUAREZ*, Hidekazu MURAKAWA** and Yukio UEDA***

Abstract

This paper examines the prediction and incorporation of residual stresses in fracture test data evaluations. In the present situation, there is several methods of allowing for residual stresses in elastic-plastic fracture mechanics, but all of the approaches imply such simplifying assumptions that could contribute to the observed scattering, and eventually produce over conservative results. Part 1 deals with the Finite Element Method analysis of Crack Tip Opening Displacement specimens of thick plates, paying special attention to the peculiarities in behavior of cracks with different lengths. Calculations of stress and strain fields, together with the shape and size of the plastic zones in front of crack tips, are presented for several load levels and crack depths. Opening displacement in the crack tip, values of the rotation factor under bending and J integrals are obtained in order to characterize the different behavior of deep and shallow cracks, when residual stresses are absent from the model. In Part 2, residual stresses will be introduced using thermal elasto-plastic FEM analysis and fracture parameters recalculated to assess their actual effect as compared with the unstressed specimen.

KEY WORDS: (Fracture) (Welding) (Toughness) (CTOD) (Residual Stress) (Finite Element Method)

1. Introduction

Crack Tip Opening Displacement (CTOD) is a widely used test for toughness assessment in weldments. It is possible to obtain accurate results for homogeneous materials but, unfortunately, for weldments a number of different factors play a role during testing, bringing about a marked scatter in the measured fracture toughness. The main influences come from: welding residual stresses, mismatching in mechanical properties and microstructural gradients. All of them take place simultaneously and their individual contributions upon the overall values are hard to discern. The Finite Element Method (FEM) is a useful tool to focus just in one of these factors, to ascertain if it is playing an important or a negligible influence on toughness figures.

The importance of welding residual stresses on fracture toughness testing is widely recognized in the literature. Nevertheless, practical difficulties to measure 3D residual stresses in thick plates prevent a further understanding and incorporation in the assessment procedures. Available methods of measurement are useful only for surface or subsurface depths (X-rays, blind hole method). Some others, among them the sectioning method supported with FEM analysis[1], are able to provide information about 3D residual stress distribution but, on the other hand, are highly time demanding both in measurement procedures and data elaboration. Usually, due to all these limitations, residual stresses are plainly not considered at all in fracture test data evaluation. Sometimes, they are assumed to have a constant value in the through-thickness direction. Beside a modeling technique to get rid of other influential factors, FEM is a powerful tool to predict residual stresses for a wide range of welding and geometrical parameters.

This paper deals with the role of welding residual stresses on the toughness of the Heat Affected Zone

† Received on July 19, 1996
* Associate Professor, Madrid Polytechnic University
** Associate Professor
*** Professor, Research Institute of Biotechnology Oriented Science and Technology, Kinki University

Transactions of JWRI is published by Joining and Welding Research Institute of Osaka University, Ibaraki, Osaka 567, Japan.

(HAZ), as measured in a CTOD test. The topic is specially meaningful for the welding of very thick plates, when high restraint levels produce transversal residual stresses that change from traction to compression through the thickness. In Part 1, the aim is to model the CTOD test, have not introduced residual stresses yet, to analyze the differences in behavior of specimens with different cracks' lengths. Stress and strain fields have been computed, and together with the shape and size of the plastic zones in front of crack tips are presented for several load levels and crack depths. The opening displacement in the crack tip, values of the rotation factor under bending and J integrals are obtained in order to characterize the differences in behavior of deep and shallow cracks. Part 2 shall be devoted to the detailed evaluation of residual stresses using a thermal elasto-plastic FEM analysis, and the behavior of the crack shall be modeled as the specimen is loaded in the presence of the residual stresses field.

Two different specimens for CTOD testing[2-4] have been proposed, **Fig.1**. The standardized specimen for lower bound fracture toughness testing is the through-thickness notched (TTN) Bx2B specimen. The BxB surface notched specimen (SN) has always been considered an alternative to TTN specimen. The main argument supporting the use of the SN specimen is that provides the most realistic geometry compared with actual cracks in structures, besides some other advantages related to experimental set up. However, surface notching yields higher CTOD values when compared to deep-notched specimens[5]. TTN provides the highest constraint and probability of sampling brittle areas because of the through-thickness notch. Moreover, crack fronts in both specimens are sampling quiet different residual stress fields. It is therefore questioned if TTN introduces an unrealistic degree of conservatism for the assessment of actual cracks in structures and components. This paper only considers the SN specimen. It is necessary to evaluate for this specimen the opening displacements at the crack tip (δ) with and without the presence of residual stresses. Otherwise, it should not be appropriate to link the differences in toughness with differences in constraint or with differences in the microstructure sampled by the crack tip.

The material, a High-Strength Low-Alloy (HSLA) steel, was selected for further comparison with previous experimental results[6]. Base material and weld metal were assumed to have both mechanical and thermal properties alike, in order to avoid the effect of mismatching on the fracture controlling parameters[7]. The microstructural gradient was not considered to focus on welding residual stresses' influence alone.

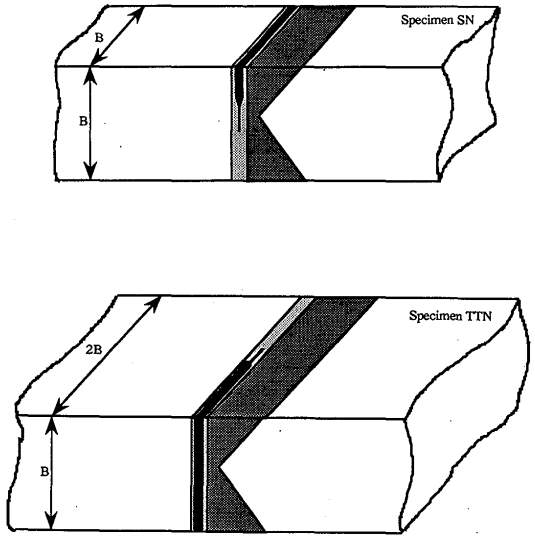

Fig.1 CTOD test specimen. Surface Notch (SN) and Through Thickness Notch (TTN) geometries.

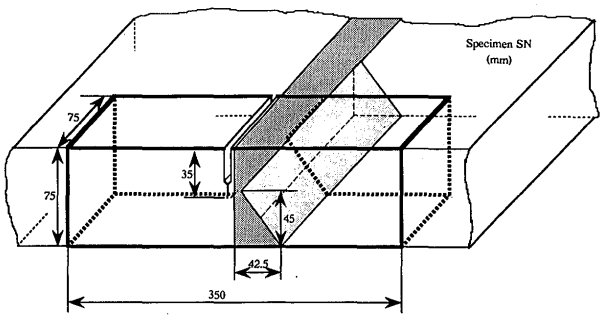

Fig.2 Extraction procedure for a CTOD specimen (SN) from a multipass weld.

2. FEM Model of CTOD Specimens

Figure 2 shows the geometry of the weld groove and the extraction procedure for the SN specimen. **Table 1** shows the mechanical properties used in the analysis; typical for a HSLA microalloyed, fine grained steel.

Table 1 Mechanical properties.

Young's Modulus, E	200.0 GPa
Yield Stress, σ_y	434.0 MPa
σ_y at Plastic Strain of 0.04	482.0 MPa
Tensile strength, σ_u	545.0 MPa

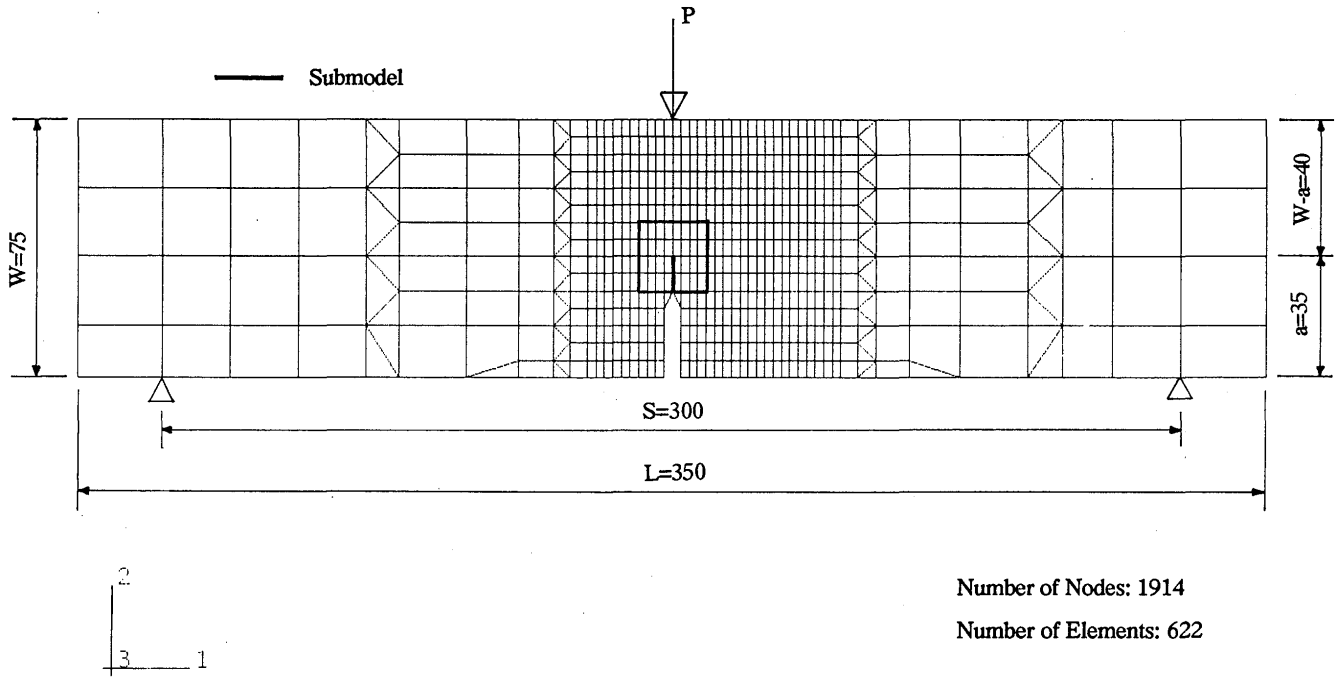

Fig.3 FEM model for the deep-notched specimen and location of the submodel boundaries.

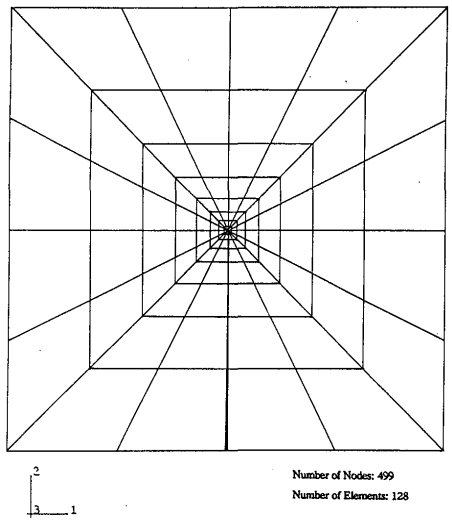

Fig.4 Focused mesh for the submodel.

The 2-D finite element model simulates a three-point bend test for both deep-notched (a/W=35/75), **Fig.3**, and shallow-notched (a/W=10/75) specimens.

The FEM analysis was conducted using the ABAQUS code. The models consisted of 10-nodes, isoparametric, rectangular elements (CGPE10). Also triangular 8-nodes elements were used (CGPE8). Last two nodes are shared by all the elements but, under the assumption of generalized plane strain, are necessary to obtain the strain in axial (welding) direction with a 2-D model. Only a linear variation in axial displacements is permitted.

In Part 2, residual stresses will be computed using the very same FEM model.

In order to obtain a proper comparison between deep and shallow cracks, loads were normalized by the plastic load for the collapse of the remaining ligament (P_y), defined as,

$$P_y=\frac{4B(W-a)^2\sigma_o}{3S} \quad (1)$$

$$\sigma_o=\frac{\sigma_y+\sigma_u}{2} \quad (2)$$

where σ_o accounts for the strain hardening and B=W for the SN specimen.

The model is not symmetric due to the presence of the weld K groove at the right side of the notch. Hence, the full model has to be used for analysis. Mesh size was a compromise to ensure two different goals: in first place, keep the degrees of freedom in a convenient number, considering that it is a highly non-linear problem, with localized plasticity and a material with temperature dependent properties (Part 2); in second place, the results have to be not determined by mesh topology, so the mesh has to be fine enough to reproduce accurately strain and stress fields in the vicinity of the crack tip. Based in similar models used by other authors[8,9] and after thoroughly checking the FEM model results against photoelastic specimens[10], the mesh size finally selected was found to be appropriated to obtain accurately the

overall deformation of the model. Nevertheless, it is necessary to use quarter point displaced nodes in the elements around the crack tip to reproduce properly the stress singularity.

This is not enough, however, to get a detailed picture of the plastic zone around the blunted crack tip. **Fig.3** shows the location and **Fig.4** the mesh used in the submodel. Another analysis was performed using this new, focused, refined mesh, and driven by displacements on the outer border of the submodel, as imposed from the results of the full model analysis. Surrounding the crack, there were 16 quarter point singular elements, with collapsed edges in the tip; this allows a fully developed plastic response of the material in the high stressed area of interest. All the nodes on the tip, sharing the same coordinates, were constrained to move together. The influence of submodel size was not investigated, but it was assured that the borders were far enough from the plastic zone at the crack tip.

The CTOD (δ) was obtained by two different approaches. Following the method based upon BS 5762[2], the values for δ were calculated from the load-CMOD (Crack Mouth Opening Displacement) curve using the expression,

$$\delta_t = \delta_e + \delta_p = \frac{K_I^2(1-\nu^2)}{CE\sigma_y} + \frac{v_p r(W-a)}{r(W-a)+a+z} \quad (3)$$

where v_p is the plastic component of the CMOD and the distance z corrects for the position of the clip gauge if attachable knife edges are used (z=0 in our model). The Stress Intensity Factor (K_I) for this specimen is,

$$K_I = \frac{PS}{BW^{\frac{3}{2}}} f\left(\frac{a}{W}\right) \quad (4)$$

and f(a/W) is a function of the crack size given by,

$$f\left(\frac{a}{W}\right) = \frac{3\left(\frac{a}{W}\right)^{\frac{1}{2}}\left[1.99-\frac{a}{W}\left(1-\frac{a}{W}\right)\left(2.15-3.93\left(\frac{a}{W}\right)+2.7\left(\frac{a}{W}\right)^2\right)\right]}{2\left(1+2\frac{a}{W}\right)\left(1-\frac{a}{W}\right)^{\frac{3}{2}}} \quad (5)$$

In **Eq.(3)**, the value of the plastic constraint factor is assumed to be C=2, and a nominal value for the rotation factor of r=0.4 has been assigned for the standard CTOD test.

The second method used to evaluate the opening, δ, was the linear extrapolation of the nodal displacements adjacent to the crack tip[11], as obtained after the detailed calculation using the submodel.

It has been also obtained the J-integral, defined by,

$$J = \int_\Gamma W dy - \int_\Gamma T_i \frac{\partial u_i}{\partial x} ds \quad (6)$$

Where W is the strain energy density, **T** is the traction vector and **u** is the displacement vector, both along the closed integration path Γ. Computation was based on the domain integral method[12], which provides rapid convergence with respect to spatial discretization. The value of J-integral is known to be mesh sensitive, so it was necessary to try several meshes for the submodel till a constant value was reached, not only for each closed integration path around the crack but also independent of further refinements of the mesh. Eight rings of elements around the crack tip were found to be enough. The two closest paths to the tip gave slightly different J values, and a constant value was reached only from the third path on. First two values were discarded and actual J value assumed to be closer to the constant value obtained for the rest of integration paths.

3. Stress and Strain Fields in Deep-notched and Shallow-notched Specimens

Figure 5 shows the load-deflection curves for the uncracked, deep-notched and shallow-notched specimens. In **Fig.6**, the load-CMOD curves for both cracked specimens are represented.

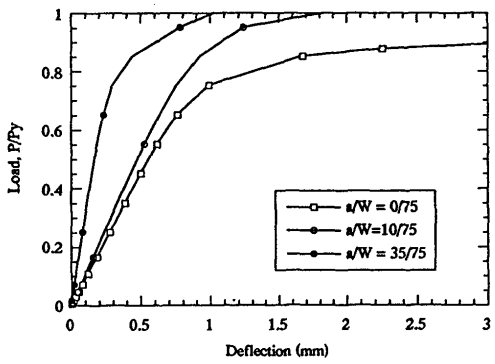

Fig.5 Load-deflection curves for the uncracked, deep-notched and shallow-notched specimens.

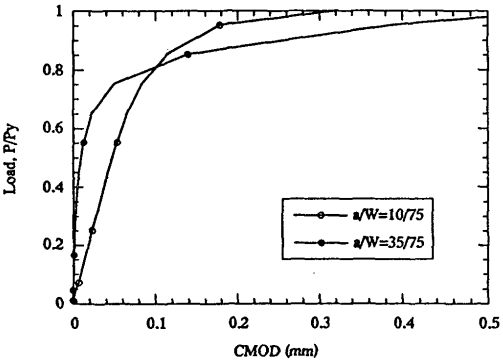

Fig.6 Load-CMOD curves for deep and shallow-notched specimens.

Figure 7 shows the crack tip opening, δ, at several load levels, as obtained from **Eq.(3)**, for a/W=35/75. The total opening, δ_t, is split in two different terms: an elastic opening, δ_e, and a plastic opening, δ_p. For normalized loads above 0.9 the plastic contribution surpasses the elastic one.

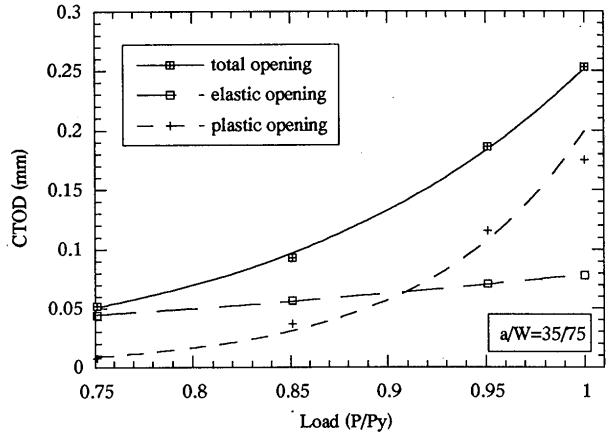

Fig.7 Crack tip opening according to BS 5762 equation.

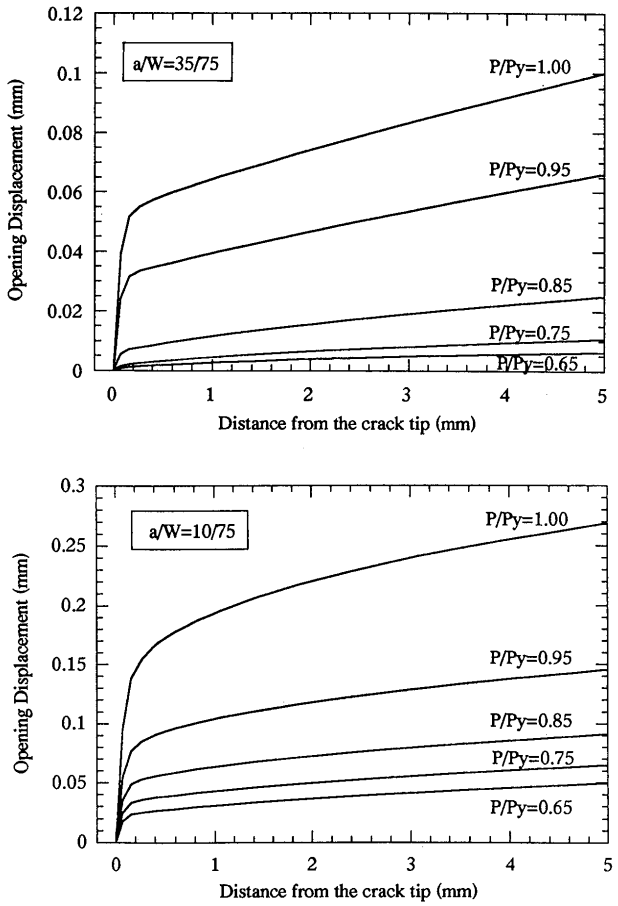

Fig.8 Lips' opening and crack tip blunting.

The opening of the crack lips for increasing loads is shown in **Fig.8**. Cracks do not just open under load but also the material around the crack tip yields, developing a blunted tip. The procedure to measure the opening at the crack tip using the linear extrapolation of the nodal displacements is outlined in **Fig.9**, and the value of δ for several loads is shown. Both δ-load curves, those of **Fig.7** and **Fig.9**, will be compared and discussed in next section.

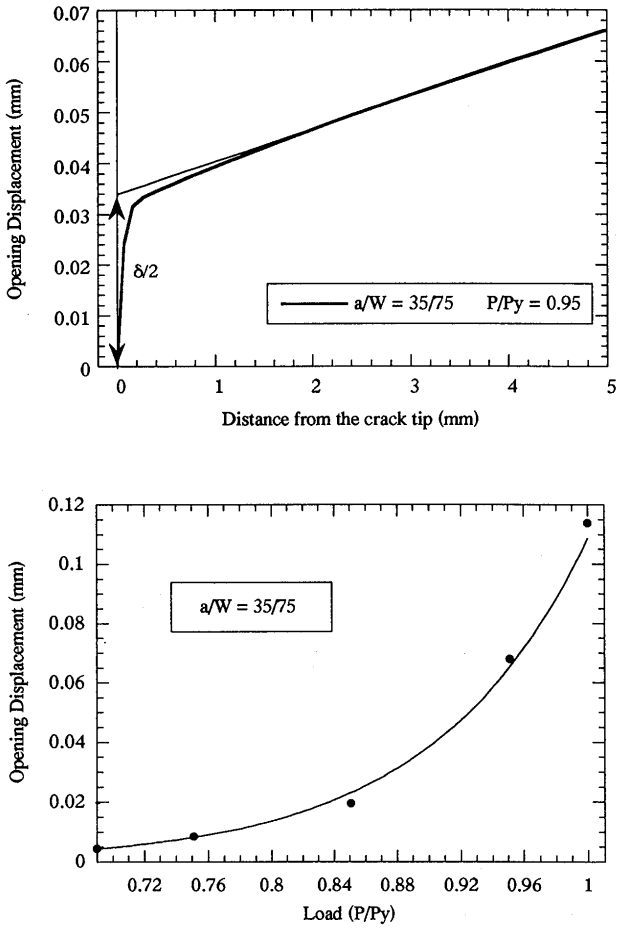

Fig.9 Procedure to measure the opening at the crack tip based on the linear extrapolation of the nodal displacements and load-opening curve.

Figure 10 shows the plastic zones in the vicinity of the crack tip, for both specimens, when the limit load is reached (P/P_y=1.0).

The opening stresses along the crack line, which were obtained from the FEM analysis at two different load levels for the deep-cracked specimen and at the same normalized load for both shallow and deep-cracked specimens, are represented in **Fig.11**. All the curves exhibit a maximum value at some distance ahead of the crack tip, because of the presence of the plastic zone.

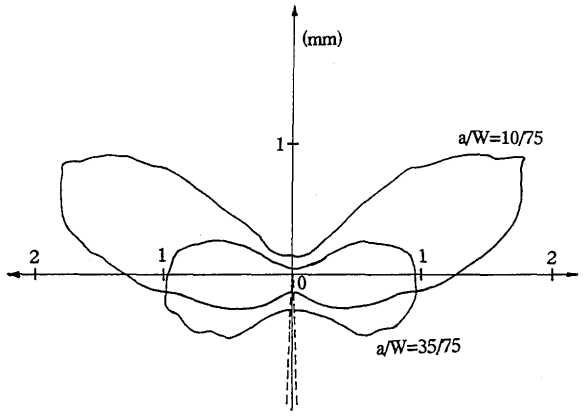

Fig.10 Plastic zones in the vicinity of the crack tips.

Figure 12 shows the values of J-integral versus normalized applied load, obtained from the FEM analysis for both types of specimens.

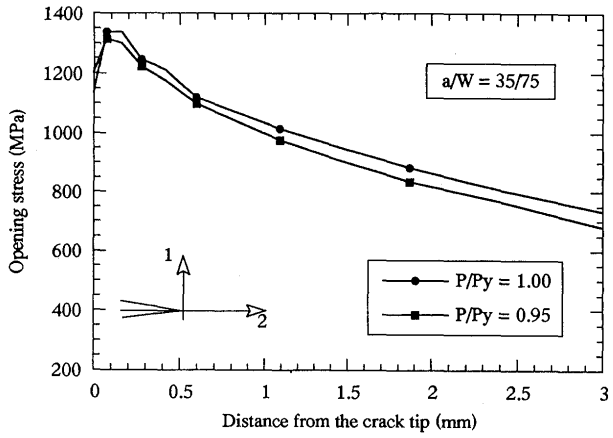

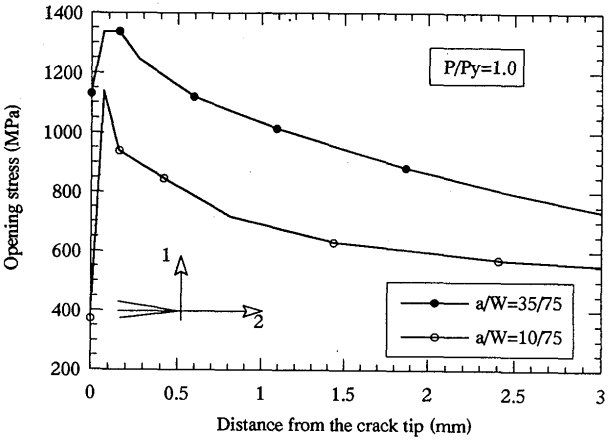

Fig.11 Opening stresses along the crack line: (a) deep-notched specimen at two different loads; (b) deep and shallow-notched specimens at limit load.

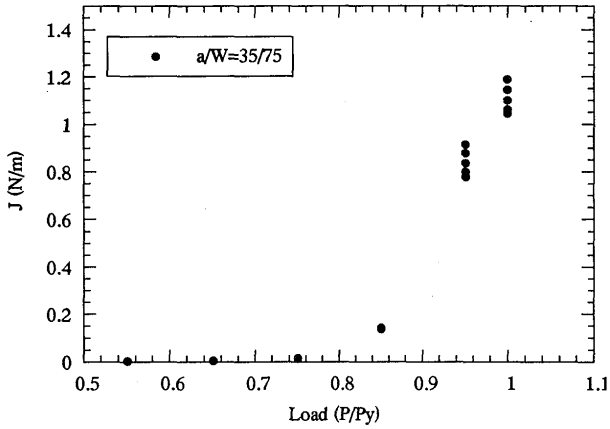

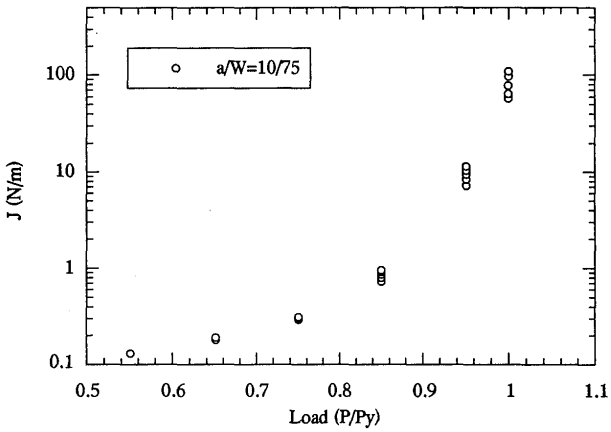

Fig.12 J-integral at limit load for deep and shallow-notched specimens.

4. Crack Size Effect on CTOD Testing

The linear extrapolation of the displacement field near the crack tip has been suggested to be time consuming and sensitive to the local displacement field[13]. Usually, it is considered enough to use **Eq.(3)** in order to obtain the value of CTOD from a remote measurement (CMOD). From the results obtained with the FEM model, both methods seem to lead to different CTOD values, as may be seen in **Fig.7** and **Fig.9**. BS 5762 assumes the plastic rotation factor to be r=0.4, that is, the crack opens using as a plastic hinge a fixed point that is located at a distance b=0.4(W-a) ahead from the original crack tip. Nevertheless, the linear extrapolation method seems to show that the plastic hinge is not a fixed point. It shifts when the load increases, as can be seen in **Fig.13** for both deep and shallow-cracked specimens. In consequence, it seems difficult to avoid the use of the extrapolation method, even if it is a time consuming procedure, to obtain a reliable value for δ.

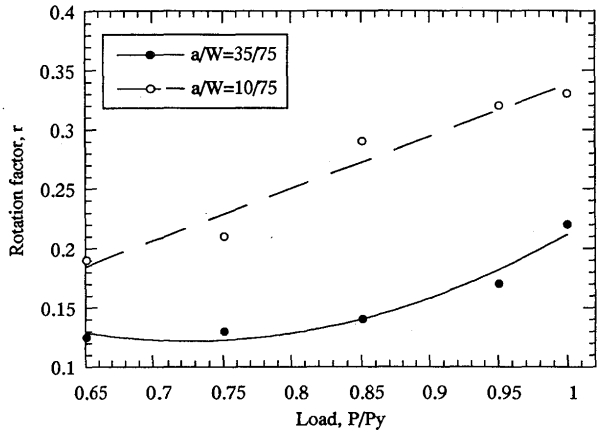

Fig.13 Shift in the location of the plastic hinge (value of the rotation factor, *r*) as the load is increased.

Let's consider the meaning of the rotation factor in a slightly different way. First, we determined, by the extrapolation method, the actual position of the plastic hinge. Then, the crack opening was measured precisely at a distance equal to b=0.4(W-a) behind this point, thus obtaining a new value for δ. The procedure is outlined in **Fig.14**. The opening displacements were obtained from BS 5762 (white symbols) and compared with the data obtained by this new procedure for every normalized load (solid black circles), resulting in a remarkably good agreement, as can be seen in **Fig.15**. The straightforward extrapolation curve (solid black squares) is far away from the other curves. The conclusion is that the most accurate values for the opening displacement at the crack tip are those obtained from the linear extrapolation method (solid black squares), because values derived from **Eq.(3)** are related to the opening displacement at different positions along the crack, and not necessarily at the crack tip, as follows from the coincidence with the values of the above proposed procedure.

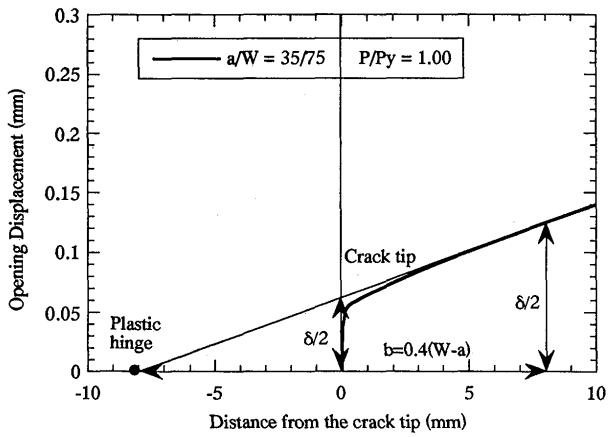

Fig.14 Crack opening measured at a distance b=0.4(W-a) from the plastic hinge, as localized by the linear extrapolation of nodal displacements.

As we are not checking this analysis against real test results, the expression 'accurate values' has to be understood in the sense that the extrapolation method always determines δ in the same position, the crack tip, whereas the equation method is based in an inconsistent assumption about the plastic hinge location, implying different positions of measurement for different applied loads or a/W ratios. These considerations are specially relevant when residual stresses are considered in the analysis (Part 2).

Usually, the value of the plastic constraint factor is assumed to be C=2. This is convenient for actual specimens, where both limit behaviors, plane stress (close to surfaces, C=1) and plain strain (inner sections, C=3), are found along the crack tip. Our model assumed a generalized plain strain state, so it could be possible to think that using a value C=3 in **Eq.(3)**, instead of C=2, a better agreement could be obtained. However, as **Fig.15** makes clear, this is a minor correction compared with the differences in *r* factor due to the shift of the plastic hinge point.

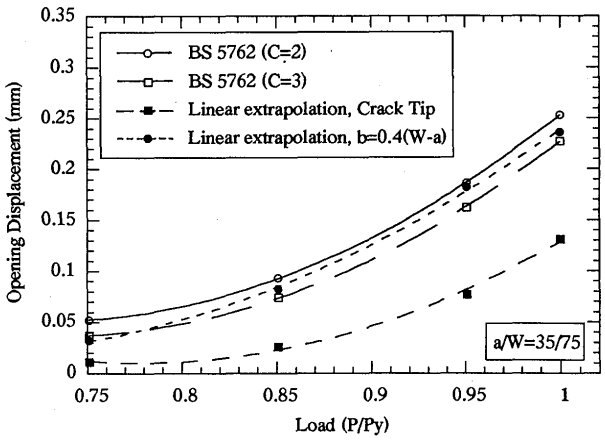

Fig.15 Crack opening by three different procedures: from BS 5762 equation, linear extrapolation of nodal displacements and a combined method.

In this sense, the new ASTM E-1290-91 standard[3] specifies different *r* values for several a/W ranges. Nevertheless, it is difficult to determine for real situations the experimental values of *r*. Some researchers[14,15] use a local measurement (δ_5), and substituting this datum in **Eq.(3)** they obtain a value of *r*=0.2 for a/W=0.1. Our values for shallow notched specimens roughly agreed with this number. However, the aim was not to obtain from the FEM model accurate values for *r*, but to compare the behavior with and without residual stresses. Using the standard value *r*=0.4 for all the loads and a/W situations would result in the smearing of the influence of residual stresses.

The shape and size of the plastic zone around the crack tip are very important features for each specimen, for plastic deformation is the main mechanism against crack propagation. Therefore, toughness value is somehow determined by the capacity of the material to develop a plastic region. As **Fig.10** shows, the computed size for the plastic zone of the deep-notched specimen resulted to be smaller than the shallow-notched's one, when bent under the same normalized loads. The impaired capacity to develop a plastic zone in deep-notched (standard) specimens justify the lower values of toughness usually obtained. This plastic constraint decreases for shallow cracks. The reason has to be found in the different stress states that evolves for each situation, as shall be discussed in next paragraph. Whatever the stress state is, welding residual stresses will change it anyhow. We will consider their influence on the size of the plastic in Part 2.

Moreover, not only the size but the shape of the plastic zone is different for both specimens. In actual situations the plastic zone will spread beyond the base material, into the HAZ and weld metal, according to its size and shape. In our model, mechanical mismatching was not considered on purpose, but usually differences in mechanical properties do have an influence on the plastic zone development. Because its shape changes for each specimen, it is also different the extent of HAZ and weld metal that is affected, which in response modified the evolution of the plastic zone.

It can be seen in **Fig.11** that the opening stress (σ_{yy}) perpendicular to the crack plane increased when the load increased; the higher the a/W ratio was, the higher the opening stress became. However, differences in fracture toughness for deep and shallow-cracked specimens can not be explained only in base to differences in σ_{yy} ahead of crack tip. Specifically in the range of a/W<0.2, for SENB specimens (TTN and SN), the influence of crack size on toughness measurement is remarkable[16]. The general effect can be explained through the use of a second parameter, which reflects the triaxiality in the stress state some small distance ahead of the crack tip. Several approaches have been proposed as, for example: the T-stress[17], the Q-parameter[18] and the Weibull stress[19] concepts. The reason has to be found in the plastic constraint in the net section of the specimen. For shallow notched specimens the plastic deformation spreads swiftly to the bottom surface, bringing about a loss of triaxiality of stress around the crack tip and, accordingly, an increased fracture toughness. The highest hydrostatic stress ahead of the crack tip is obtained when a/W=0.5, the standard specimen, and hence conservative toughness values are guaranteed. This situation could change in the presence of residual stresses, and shall be analyzed in Part 2.

5. Conclusions

The importance of welding residual stress on fracture toughness testing is widely recognized in the literature. Nevertheless, it is not an easy task to incorporate its presence to the toughness assessment procedures for weldments. There are mainly two reasons: in first place, others influential factors (mismatching and microstructural gradients) take place simultaneously and their individual contributions upon the overall values are hard to discern; in second place, the actual measurement of 3D residual stresses in thick welds is difficult and time consuming. The FEM modeling allows to analyze individually the effect of residual stresses and sheds some light on the understanding of their role.

A FEM analysis of CTOD specimens in multipass weldments of thick plates has been conducted. As a first step in the research, residual stresses have not been introduced in order to clarify the differences in behavior of deep and shallow-notched specimens. Otherwise, these differences would result in the smearing of the true significance of residual stresses. Some conclusions have been drawn:

(1) Standard procedures to obtain the crack tip opening displacement from remote measurements (CMOD) and the values computed from linear extrapolation of displacements in the vicinity of crack tip do not yield the same values. The difference seems to be that whereas the conventional procedures assume a rotation factor that keeps constant for every normalized load and crack depth, the extrapolation procedure shows that the plastic hinge is constantly shifting as the load is increased or the geometry changed.

(2) The size and shape of the plastic zone ahead of the crack tip are different for deep and shallow-notched specimens, when bend under the same normalized loads. The plastic zone for the deep-notched specimen (a/W=35/75) is smaller than for the shallow-cracked (a/W=10/75). This impaired capacity to develop a wider plastic zone, due to the stress state in the vicinity of the crack tip, justify the lower values of toughness usually obtained for the deep-notched specimen. The plastic constraint decreases as the crack depth decreases.

(3) Both the shift of the plastic hinge and the size and shape of the plastic zone are closely related to the toughens measured after a CTOD test. It is necessary to consider how the welding residual stresses modify

such parameters during the fracture test. This results will be presented in Part 2.

References

1) Y. Ueda and N.X. Ma, "Measuring Methods of Three Dimensional Residual Stresses with Aid of Distribution Function of Inherent Strain", Transactions of JWRI, 24-2, 1995, 123-130.
2) British Standard 5762, "Methods for Crack Opening Displacement (COD) Testing", British Standard Institution, London 1979.
3) ASTM E 1290-91, "Standard Test Method for Crack-Tip Opening Displacement (CTOD) Fracture Toughness Measurement", American Society for Testing of Materials, 1991.
4) EGF P1-90, "Recommendations for Determining the Fracture Resistance of Ductile Materials", European Group on Fracture, 1989.
5) C. Thaulow, M. Hauge, A. Larsen, F. Minami and M. Toyoda, "Effect of Extraction Procedure on the Fracture Behaviors of HAZ-notched Welded Joints", 2nd Workshop on Constraints Effects on the Structural Performance of Welded Joints, September 1st, 2nd, 1994, Osaka, Japan.
6) J.C. Suárez, F. Molleda, R. González and R. Jiménez, "Correlation of Modified Crack Tip Opening Distance with Heat Input to the Heat Affected Zone of High-strength Low-alloy Steels", Theoretical and Applied Fracture Mechanics, Vol. 21, 1994, 17-22.
7) M. Toyoda, "Significance of Mis-matching of Steel Welds", Proc. of the Workshop on Strength Mismatching and its Control, M. Toyoda (Ed.), July, 1992, Tokyo, Japan, 121-133. IIW Doc. X-1254-92.
8) D.S. Kim, C.L. Tsai, J.Liao and J. Papritan II, "Evaluation of Local Brittle Zones Using the Finite Element Method", Welding Journal, Welding Research Supplement, November, 1994, 257s-264s.
9) F. Minami, M. Ohata and M. Toyoda, " Prediction of Specimen Geometry Effect on Fracture Resistance of HAZ-notched Welds by the Local Approach", 2nd Workshop on Constraint Effects on the Structural Performance of Welded Joints, M. Toyoda (Ed.), September 1-2, 1994, Osaka, Japan, 1-10. IIW Doc. X-1300-94.
10) J.A. Martínez, J. Espona and J.C. Suárez, "Comparative Study between Photoelastic and Numerical Methods for Stress Analysis of Welding Defects", Anales de Mecánica de la Fractura, Vol. 12, 1995, 55-60 (in Spanish).
11) C.L. Tsai, D.S. Kim and J. Papritan II, "Analysis of Fatigue Crack Propagation Behavior in Fillet Welded T-joints", Welding Journal, Welding Research Supplement, 70(6), 1991, 150s-155s.
12) C.F. Shih, B. Moran and T. Nakamura, "Energy Release Rate along a Three-dimensional Crack Front in a Thermally Stresses Body", International Journal of Fracture, 30, 1986, 79-102.
13) D.S. Kim, C.L. Tsai and J.Liao, "Simulation of Crack Propagation for the Local Brittle Zone of Welded Joints", 5th. International Symposium of the Japan Welding Society, 1990.
14) M. Koçak, S. Yao, K-H. Schwalbe and F. Walter, "Effect of Crack depth (a/W) on Weld Metal Fracture Toughness", International Conference Welding 90, Geesthacht-Hamburg, Germany, 1990, 255-268.
15) I. Rak, M.Koçak and B. Petrovski, "Fracture Toughness Evaluation of Repair Welded Joints for Offshore Application", Welding in the World, Vol. 33, No. 3, 1994, 168-177.
16) M. Toyoda, "Fracture Toughness Evaluation of Steel Welds (Review Part II)", Osaka University, 1989, 88-91.
17) J. Sumpter and J.W. Hancock, "Shallow Crack Toughness of HY80 Welds: a Analysis based on T Stress", International Journal of Pressure Vessels and Piping, 45, 1991, 207-221.
18) C.F. Shih and N.P. O'Dowd, "A Fracture Mechanics Approach based on a Toughness Locus", Proceedings of the International Conference in Shallow Crack Fracture Mechanics, Toughness Test and Applications, Cambridge, 1992.
19) F. Mudry, "A Local Approach to Cleavage Fracture", Nuclear Engineering Design, 105, 1987, 65-76.